



İhsan Kırık

Bingöl University, alihsankirik@gmail.com, Bingöl-Turkey

Derya Abak

Bingöl University, dabak902@gmail.com, Bingöl-Turkey

DOI	http://dx.doi.org/10.12739/NWSA.2022.17.1.2A0187	
ORCID ID	0000-0002-8361-319X	0000-0001-9862-7888
Corresponding Author	İhsan Kırık	

FRICION WELDING OF AISI 1020 WITH RAMOR 500 STEEL: MICROSTRUCTURE, TENSILE AND FATIGUE STRENGTH

ABSTRACT

The joint of dissimilar materials like Ramor steel and low carbon steel is very important for defense industry in term of improve functionality of components and enhance the working limits. In this study, Ramor 500 and AISI 1020 steel, which are widely used in the defense industry, were joined using the continuous driven friction welding method and the effects of production parameters on the joint micro structure and mechanical properties were investigated. SEM, EDX, X-Ray and Hardness analyzes were performed for macro and microstructure analyses. According to the tensile test results, the rotary bending fatigue test was also used to determine the mechanical properties. As a result, the correct selection of production parameters is of great importance for joining Ramor 500 and AISI 1020 steel with different properties. Tensile strengths and fatigue strength were increased compared to main materials.

Keywords: Ramor 500, Friction Welding, Tensile Strength, Fatigue, Fractography

1. INTRODUCTION

According to the carbon content of armor steels, it is in the class of low carbon steels. In terms of chemical composition, a tempered and quenched steels like armor are used in protection of civil and military vehicles, because of their high protective properties [1, 2, 3, 4, 5 and 6]. In order for armor steels to be resistant to penetration, it is desirable to have great hardness and resistance. But above 600 Vickers hardness, sheet material will encounter brittle fracture during impact. Resistance to ballistic impacts is provided with great toughness. Apart from this, it is very necessary to keep production difficulties such as cutting, weldability and formability to a minimum. Chemical composition and thermal process conditions are very important in order to obtain the said capabilities of armor steels. In this context, joining of armor steels with traditional fusion welding is not preferred due to the metallurgical negativities occurring in the weld area and the loss of armor properties of these steels. In order to prevent the armor steels from losing their protective properties when welded with different steel, friction welding, one of the solid state welding techniques was preferred because the joint area is very narrow and the temperature of this area is below the melting temperature of the joint materials [7, 8 and 17].

Kırık (2015) joined Ramor 500 and AISI 1040 steel using diffusion welding with different temperatures and investigated the effects of the joining temperature on the microstructure. It was determined that the diffusion welding temperature had a significant effect on the bond

How to Cite:

Kırık, İ. and Abak, D., (2022). Friction Welding of AISI 1020 with Ramor 500 Steel: Microstructure, Tensile and Fatigue Strength. Technological Applied Sciences, 17(1):39-52. DOI:10.12739/NWSA.2022.17.1.2A0187.



quality and the highest strength was 920MPa in the joint using 900°C, 3MPa pressure and 30 minutes.

Sarsılmaz et al. (2017) joined Ramor 500/AISI 2205 stainless steels by the friction welding method using variable parameters such as friction time and friction pressure and reported that the highest tensile test result was obtained as 1020 MPa.

Merzali (2013) studied the homogenization of the phase properties of the almost unchanged and tempered areas in the area under the heat effect after welding of the armor steel and the suitability of the mechanical properties. He used the light microscope for microstructural studies. First, heat treatment variables were developed to obtain the same structure and hardness parameters on the original armor steel. With the heat treatment variables made in armor steel, it has achieved the same hardness and phase properties as the original armor steel. After welding, the structure was divided into regions determined by considering the literature, and its microstructural and mechanical properties were examined.

Bekçi (2021) investigated the ballistic performance of Ramor 550 armor steel plates against 7.62mm bullets in various conditions, both experimentally and numerically. It was concluded that the ballistic strength of the plates increased with increasing tilt angle. In the numerical analysis part, inclined plate structures were examined. It has been observed that the finite element analyzes carried out highly reflect the test results.

Metallic materials with different properties create some negative results when combined with fusion welding methods [11, 12, 13 and 18]. In particular, Ramor steels, which serve as armor, may lose their armor properties in the welding zone and heat affected zone [14, 15 and 16]. For this purpose, Ramor 500 steel, which has different types in the defense industry and using in many armored vehicles, and with AISI 1020 steel, which has good weldability, are combined with friction welding method, which provides superior advantages. After the welding process was completed, mechanical (tensile and fatigue) experiments and microstructural examinations were carried out.

2. RESEARCH SIGNIFICANCE

Ramor 500 armor steel, which is widely used in the defense industry, and AISI 1020 low carbon steel were combined using friction welding method. Ramor 500 steel is supplied in plate form and processed into bars with a diameter of 12mm and AISI 1020 steel, were successfully joined without any errors using different process parameters by friction welding. Using the lowest friction time with higher friction pressure and rotation speed increases the tensile strength. The fatigue and tensile strengths of specimens joined using 1800rpm rotational speed increased with increasing friction time, but the friction time required for joining quality decreased with increasing rotational speed (2200rpm) and friction pressure (60MPa).

Highlights:

- Ramor 500 armor steel, which is widely used in the defense industry, and AISI 1020 low carbon steel were combined using friction welding method.
- Ramor 500 steel is supplied in plate form and processed into bars with a diameter of 12mm and AISI 1020 steel, were successfully joined without any errors using different process parameters by friction welding.
- Using the lowest friction time with higher friction pressure and rotation speed increases the tensile strength.

3. MATERIAL AND METHOD

3.1. Materials

AISI 1020 steel and Ramor 500 steels used in the friction welding process are commercially available. The chemical contents of commercially available materials are given in Figure 1 Ramor 500 and Figure 2 AISI 1020 steel. Ramor steel was bought in the market in the form of plates in the size of 300x72x12mm and cut into 12x72mm dimensions using a band saw and coolant, then it was brought to $\varnothing 12 \times 72$ mm bar dimensions by the lathe. Commercially purchased AISI 1020 steel in $\varnothing 12$ mm bars was cut using a band saw with coolant and in $\varnothing 12 \times 72$ mm dimensions.

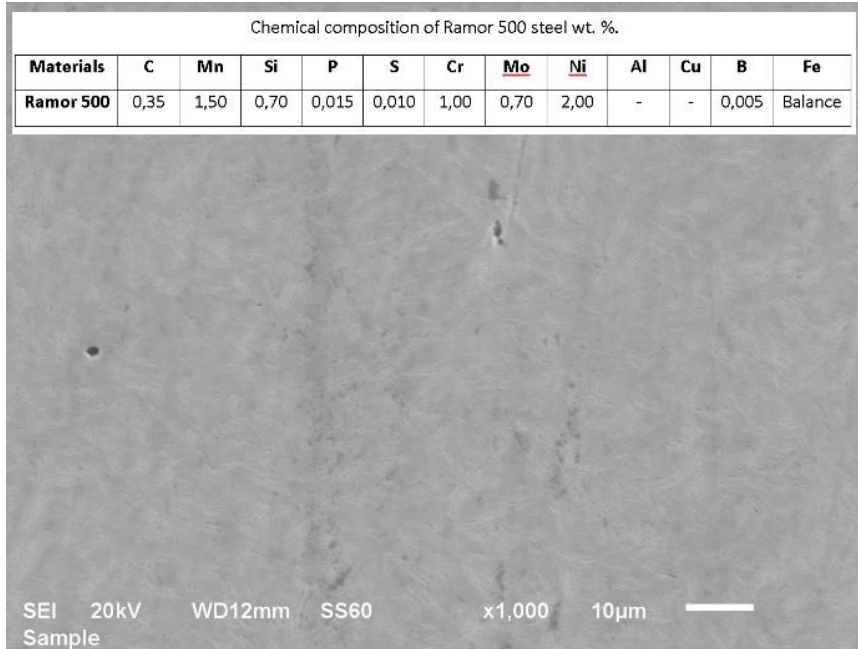


Figure 1. The SEM photo and chemical composition of Ramor 500 steel (wt.%)

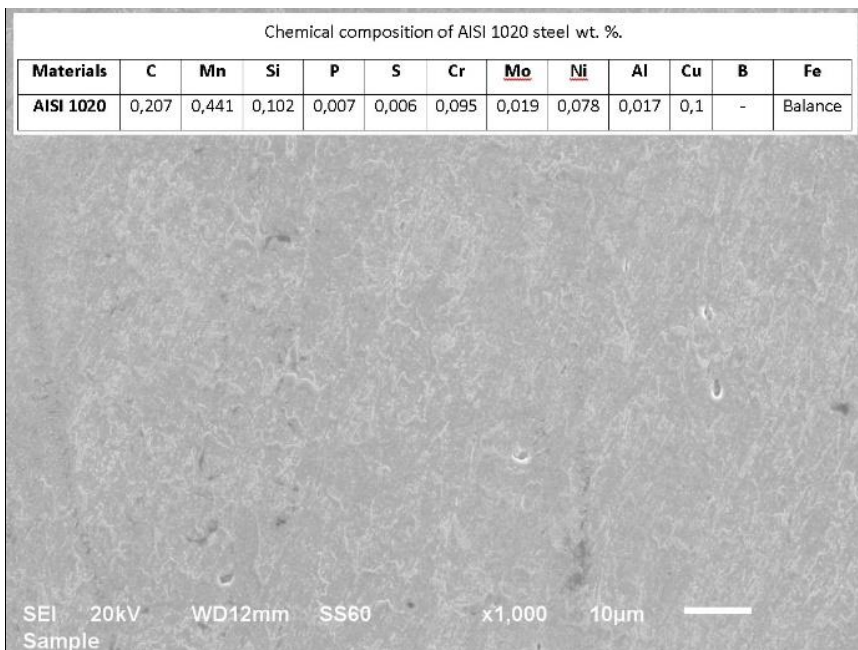


Figure 2. The SEM photo and chemical composition of AISI 1020 steel (wt. %)

3.2. Friction Welding

As a result of the literature review; process parameters such as rotation speed, friction pressure and friction time, which have a great effect on the microstructure and mechanical behavior of the joints made with friction welding, were chosen as variables [19, 20, 21 and 22]. These variables were determined as two different rotation speed, two different friction pressure and three different friction time and examined in the experimental program in the order given in Table 1. Friction welds were made in the orientation shown in Figure 3 a-b in a PLC controlled continuous drive friction welding machine.

Table 1. Friction welding parameters used for the production of welded joints

Sample No	Rotation Speed (rpm)	Friction Time (s)	Friction Force (MPa)	Yield Force (MPa)	Yield Time (s)
S1	1800	6	40	100	12
S2	1800	8	40	100	16
S3	1800	10	40	100	20
S4	2200	6	40	100	12
S5	2200	8	40	100	16
S6	2200	10	40	100	20
S7	2200	6	60	120	12
S8	2200	8	60	120	16
S9	2200	10	60	120	20

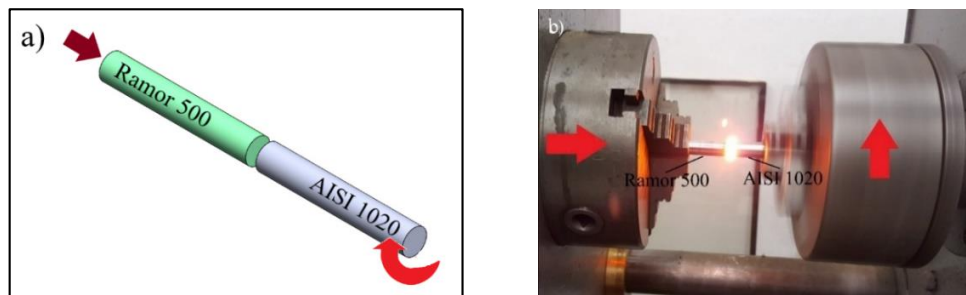


Figure 3. a) Attachment of Ramor 500 and AISI 1020 steel to chucks
 b) Application picture of friction welding

3.3. Microstructure Tests

To observe the structural change in the joint area of the samples after the welding process, the samples were cut perpendicular to the joint surface as seen in Figure 4, smoothed with 80-1200 mesh sandpaper, and polished with 3 μm diamond paste. SEM and EDS analyzes were performed to determine the structural transformations in the intermediate regions of the friction welded samples. The sample S1 which has the lowest speed, friction pressure, and friction time, S5 with medium values, and S9 with the highest value were chosen in this study to explain the interaction of the joint zone more simply.

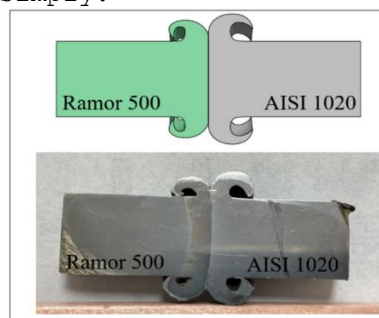


Figure 4. Schematic representation of the microstructure sample

3.4. Microhardness Analyses

Microhardness measurements were taken after welding to determine the hardness change in the joint area of the samples. The microhardness area were depicted in schemas as shown between A and B (10mm) points as shown in Figure 5. Microhardness measurements were taken with the AOB brand microhardness apparatus in the Central Laboratory of Bingol University using the Vickers (Hv) unit with 0.5mm intervals under a 20gr load.

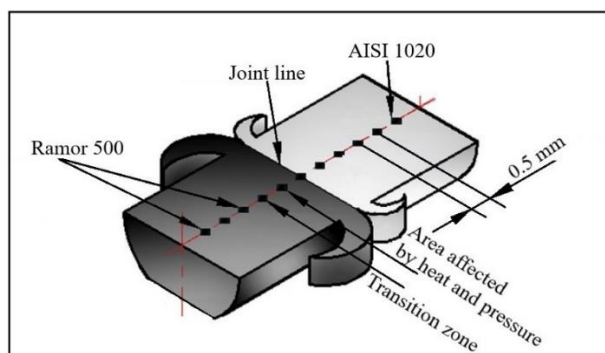


Figure 5. The depicted of points where microhardness was measured [23]

3.5. Tensile Test

Tensile tests were performed on the joints to determine the greatest stress values of the samples welded by friction welding. The tensile samples were made accordance with ASTM E8 standard as seen in Figure 6. Tensile tests were performed at a tensile speed of 1 mm*min⁻¹ using a SHMADSU tensile device with a load capacity of 50000 N. The average measured maximum tensile stress values of Ramor 500 and AISI 1020 steels used in this study were measured as 1680 and 608 MPa, respectively.

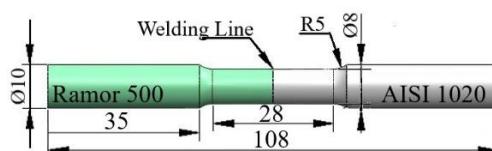


Figure 6. The sample dimensions used in the tensile test (mm)

3.6. Fatigue Test

Many materials used in the industrial field are exposed to continuous stress or deformations below the tensile strength. For this reason, the applicability of materials can be better judged by their fatigue properties [23]. It is known that there are micro-defects in the joints of the welded materials and these defects cause fatigue damage in the later stages [13]. Furthermore, fatigue damage at welded connections has been observed at the weld zone joint regions, the welding start and finish points, and the fatigue life could vary depending on the components of the local strains [5]. For this reason, the fatigue limit of friction welded joints with different production characteristics was determined with a fatigue rotary bending machine. The fatigue tests were carried out at various loads on a rotary bending test machine. For fatigue tests, samples were prepared according to the ASTM E466 standard in the form of toroids with the smallest diameter of 4mm (see in Figure 8). Fatigue tests were carried out according to tensile values which determined in the range of %30-70 percent of the tensile strengths. Wohler Curve (S-N) of AISI 1020 and Ramor 500 steels were given in Figure 7a and b, respectively.

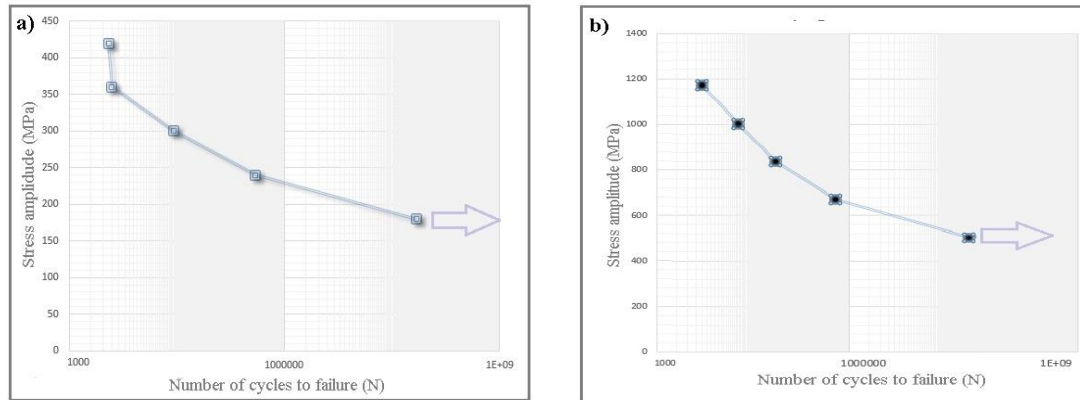


Figure 7. a) S-N diagram of AISI 1020, b) S-N diagram of Ramor 500

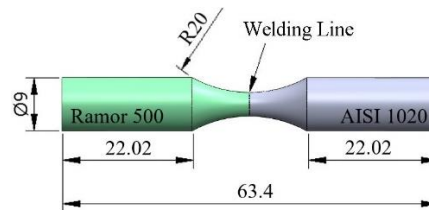


Figure 8. Specimen sizes for fatigue tests (mm)

4. RESULT DISCUSSION

4.1. Macro and Microstructure Examination

Since the materials joined by friction welding are under the effect of axial pressure and friction, the material overflowing from the welding interface forms a flange and the lengths of the joined materials are shortened. The changes in the surface and protruding material profiles of the samples combined using different processing parameters are given in Figure 9 a-c. The areas of the welded connections that are affected by heat and pressure are critical in terms of joint quality. Furthermore, the areas affected by heat were clearly visible on both sides of AISI 1020 and Ramor 500, because their heat transmission coefficients are not very different. While the lengths of the parts shorten, the amount of material overflowing from the contact surface and flange diameters increase as a result of friction welding parameters as can be seen in Table 2. When we look at the macro pictures of the samples joined using 1800 rpm (Figure 9b), it is seen that the low rotation speed and friction time are not sufficient to reach the plastic deformation required for the joining, as can be clearly seen in the sample no S4. Except for the samples numbered S4, rotation speed, friction pressure and friction time used in all samples appear to be appropriate. The amount of flanged material and the lengthening of the combined samples were completely different, because of the difference in heat flux coefficients. As a result of this difference, the length shortening of Ramor 500 steel was less according to than of AISI 1020 steel (Table 2). There are no gaps, cracks or incorrect weld joint design at the connection surface of the samples as shown in the SEM photos in Figure 10a-c. From the SEM images of the samples with different processing parameters, it was seen that the coalescence was very good and there were microstructures close to each other. EDS analysis of sample S9 is given in Figure 11. As seen in the figure, the carbon ratio of the welded area was measured as 2.031. It has been observed that the element concentration of the joint zone is compatible with the element concentration of the joined materials.

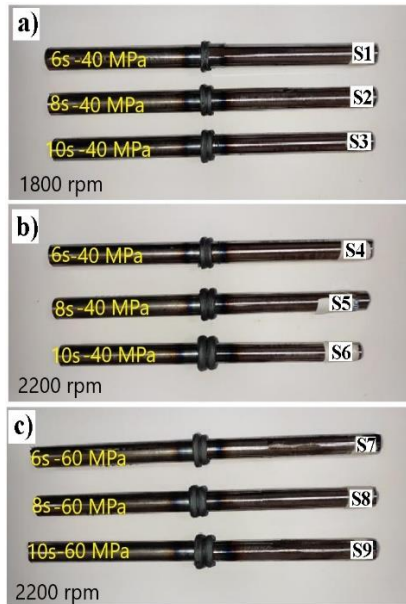


Figure 9. Macro photograph of friction welded samples
 a) S1, S2 and S3 b) S4, S5 and S6, c) S7, S8 and S9, respectively

Table 2. Average length shortening and flange diameters of AISI 1020 and Ramor 500

Sample No	Length shortening AISI1020 (mm)	Flange diameter AISI1020 Ø (mm)	Length shortening Ramor 500 (mm)	Flange diameter Ramor 500 Ø (mm)
S1	5.80	16.90	2.00	16.00
S2	7.10	18.35	5.15	17.20
S3	11.85	20.00	6.45	18.80
S4	6.60	16.00	1.80	15.00
S5	6.90	17.10	3.25	15.75
S6	8.00	17.45	3.20	16.10
S7	6.85	18.00	4.90	16.00
S8	8.60	18.60	5.85	16.85
S9	13.90	18.45	6.85	21.00

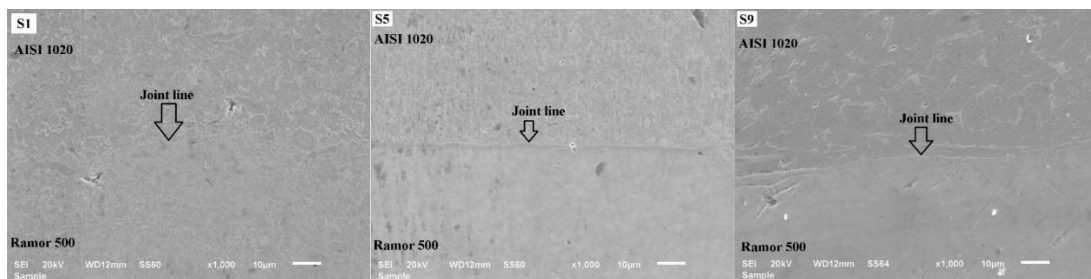


Figure 10. SEM images of S1, S5 and S9 samples

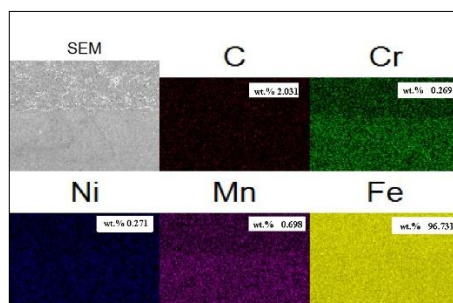


Figure 11. EDS analysis of joint line of S9 sample

4.2. Examination of Microhardness Measurement

The microhardness measurement results of the friction welded joints made using two different rotational speeds, friction pressures and friction times, made with 0.5 mm intervals along a linear line from A and B point in the joint center to the base metal, are shown in Figure 12. The distribution of microhardness changes in four areas. When the hardness profile of sample S1 is examined; It is seen that the hardness in the RAMOR 500 region is maximum 589.3 Hv and decreases from the intermediate region towards Ramor 500 steel. As a result, the width of the heat and pressure-affected zones (HPAZ) changes. Previous research has found that the best hardness values occur in areas influenced by heat, such as in the friction joint line [8, 17 and 23].

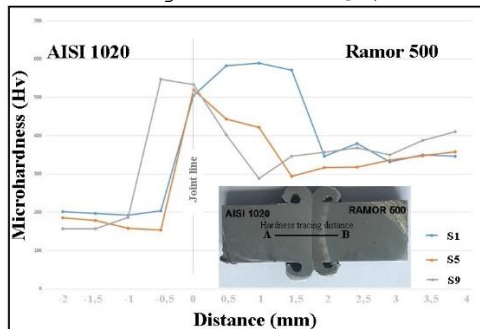


Figure 12. The Microhardness distribution of S1, S5 and S9

4.3. The Properties of Tensile Test

Tensile testing was performed on the main materials used in the tests (Ramor 500 and AISI 1020), as well as the friction welded samples, and the results are shown in Figure 13. The tensile results of friction welded joints were found to be close to the tensile strength of AISI 1020 steel. Specimen no S7 had a maximum tensile stress of 604MPa, while specimen no S1 had a minimum tensile stress of 468MPa. The tensile strengths improve as the number of cycle increases from 1800 to 2200, but the samples joined with 1800 rpm and different friction times show similar results as the friction time increases. On this basis, it can be concluded that the friction time of Ramor 500 steel and AISI 1020 steels is more effective in friction welding than the number of revolutions. The tensile strength values were also increased when the friction pressure was increased from 40MPa to 60MPa for the samples joined with 2200rpm. The reason why the lowest strength is seen in the S1s that both the friction pressure (40MPa) and the number of cycle (1800rpm) is low to eliminate the mixture band from contact surfaces of samples. The samples with the highest, medium and lowest tensile strengths were examined for fracture surface morphologies. Brittle fracture was observed in S1 sample joined at low speed and low friction pressure (Figure 14). While ductile-brittle fracture (mixed fracture) was observed in sample S5 (Figure 15), ductile fracture behavior was observed in sample S9 on the side of the AISI 1020 base material (Figure 16).

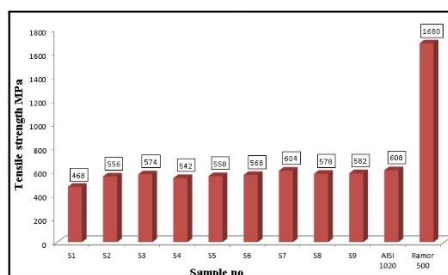


Figure 13. The tensile test results of friction welded joints

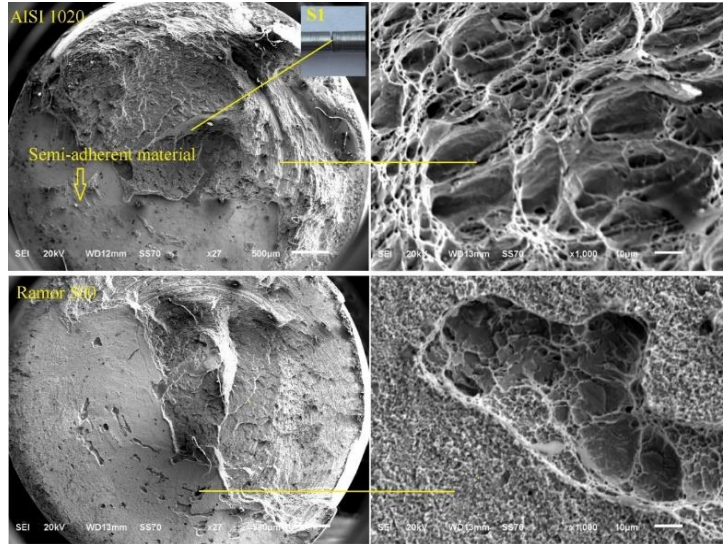


Figure 14. SEM photograph of the sample S1 after the tensile test

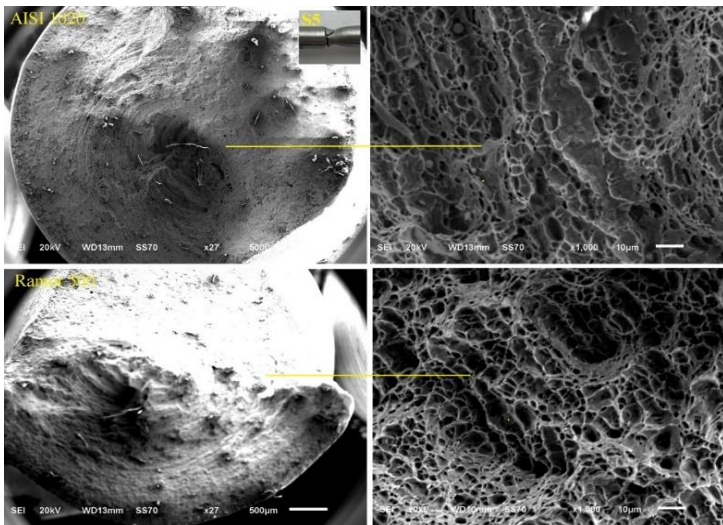


Figure 15. SEM photograph of the sample S5 after the tensile test

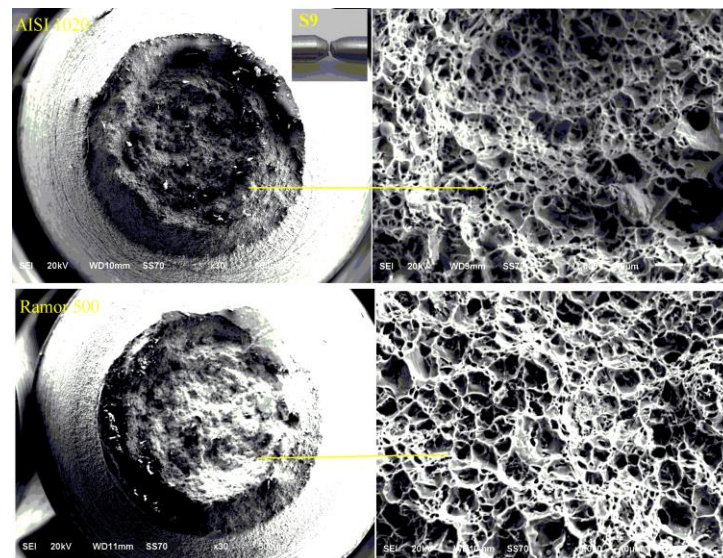


Figure 16. SEM photograph of the sample S9 after the tensile test



4.4. Fatigue Test Analyses

While cracking due to fatigue is possible in armor steels, it is uncommon in practice because of armored structures are typically overdesigned from a fatigue standpoint. Fatigue is usually linked to poor weld joint design, which results in complex residual stresses with dynamic loads that are either unpredicted non-design loads or occur over a longer period than a reasonable service life [5]. The fatigue strength of S1, S2 and S3 samples were depicted in Figure 17. The fatigue strength of sample S1 was lower than samples S2 and S3 at 420MPa applied loads. The fatigue strength of three samples are close to AISI 1020 steel and each other. However, the increase in load causes a parallel change in fatigue strength. When examined for these three samples, it is seen that the quality of joints can be increased by increasing the friction time. Figure 18 shows the Wohler curves of the S4, S5, and S6 samples which joined with different friction times (6, 8, and 40 s), 2200rpm rotation speed and 40MPa friction pressure. These samples' fatigue limits are estimated between 180 and 250MPa. When the Wohler curve in Figure 1x is evaluated, the fatigue limit increases little as the friction time increases. The number of cycles have a significant impact on the friction welded joint as is well known [7 and 23]. The heat of the contact surface rises in tandem with the increase in cycle number. It is important in eliminating the pores, voids and micro defects that appear in the material that softens with the effect of heat on the contact surfaces under axial pressure. In addition to other properties, increasing rotation speed improves fatigue strength and tensile strength [17].

S-N curves of S7, S8 and S9 samples are given in Figure 19 by keeping the number of revolutions constant and increasing the friction pressure from 40 MPa to 60 MPa and using three different friction times (6, 8 and 10s). The specimen S7, which was joined with 2200 rpm rotation speed, 60 MPa friction pressure and 6 second friction time had the highest fatigue strength. Among the all specimens, the S7 specimen has the highest fatigue strength. As a result, maximum rotation speed, suitable friction pressure and minimum friction time are the most suitable parameters for joining AISI 1020 and Ramor 500 with friction welding.

After fatigue test the fracture surface pictures of the samples S1, S5 and S9, which were joined using low, medium and high parameter values, are given in figures 1, 2 and 3, respectively. When viewing the SEM images of sample S1, it is clear that the fracture begins at the joint center and spreads outward (see in Figure 20). However, in samples S5 and S9, the fracture appears to begin at the surface and progress inward (see in Figure 21 and 22). When the macro-and micro-structure broken surface and SEM images of the samples S1, S5 and S9 are examined together. When there is no welding error or material defects, fatigue damage occurs mostly on the surface. The fatigue cracks began on the surface of the S5 and S9 samples. The fatigue fracture propagates from the inside out in the combined sample with low parameters, but the fracture propagates inward from the surface in the samples with medium and high parameters.

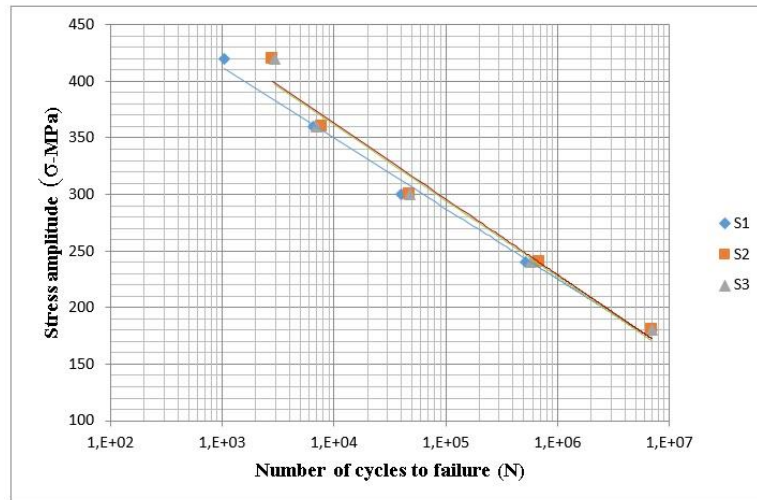


Figure 17. Wohler curves (S-N graph) of the friction welded samples (S1, S2 and S3)

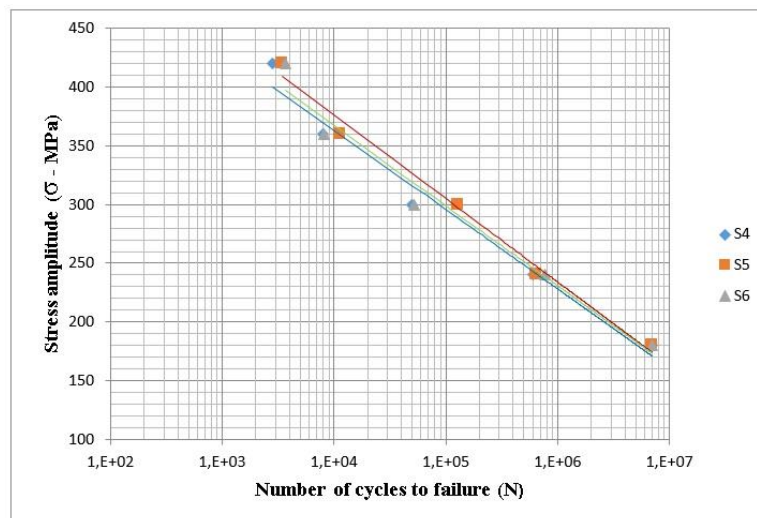


Figure 18. Wohler curves (S-N graph) of the friction welded samples (S4, S5 and S6)

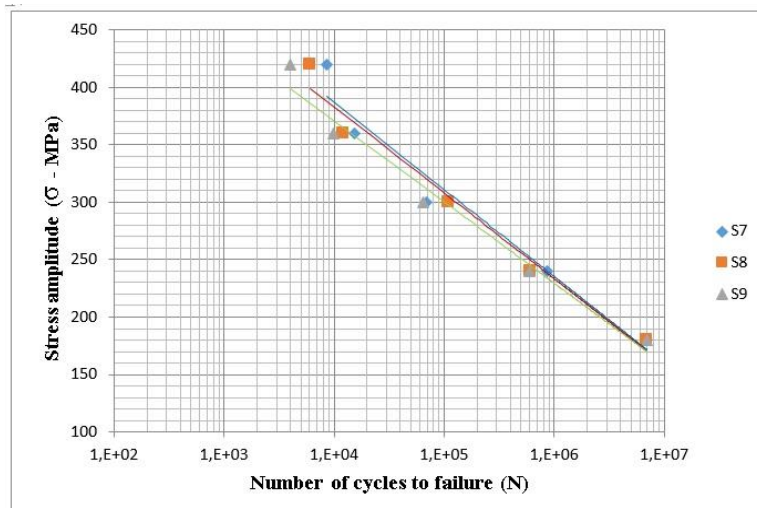


Figure 19. Wohler curves (S-N graph) of the friction welded samples (S7, S8 and S9)

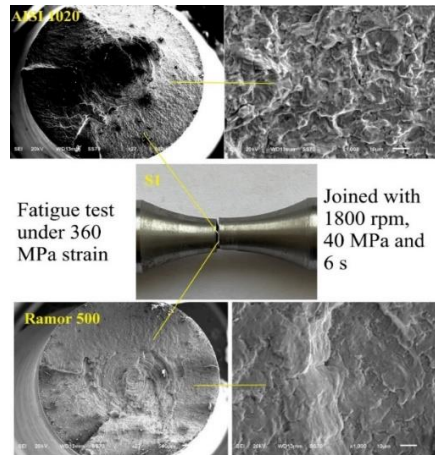


Figure 20. Fractography and failure analysis of the S1

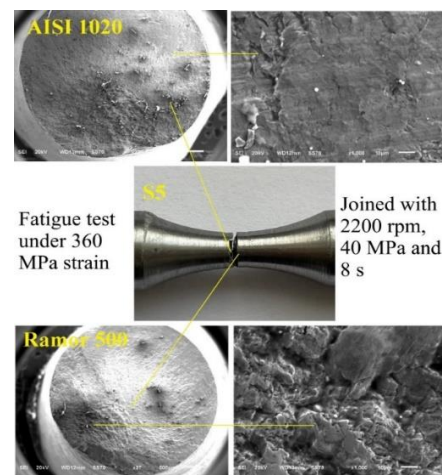


Figure 21. Fractography and failure analysis of the S5

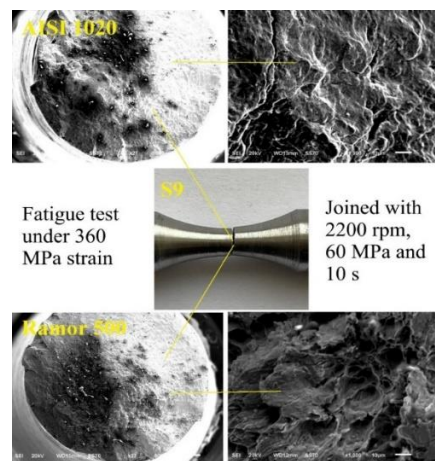


Figure 22. Fractography and failure analysis of the S9

5. CONCLUSIONS

In this study, Ramor 500 armor steel, which is widely used in the defense industry, and AISI 1020 low carbon steel were combined using friction welding method and the following results were obtained.

- Ramor 500 steel which are supplied in plate form and processed into bars with a diameter of 12mm and AISI 1020 steel, were successfully joined without any errors using different process



parameters by friction welding. But, the low cycle number and friction time are not sufficient to reach the plastic deformation required for the joining.

- Using the lowest friction time with higher friction pressure and rotation speed increases the tensile strength. The tensile results of friction welded joints were found to be close the tensile strength of AISI 1020 steel. Specimen no S7 had a maximum tensile stress of 604 MPa, while specimen no S1 had a minimum tensile stress of 468 MPa.
- The fracture occurred at the weld center of the S1 sample, at an angle of 45 degrees to the weld area in the S5 sample, but at the outside of the weld area in the S9 sample, on the AISI 1020 side.
- The fatigue and tensile strengths of specimens joined using 1800 rpm rotational speed increased with increasing friction time, but the friction time required for joining quality decreased with increasing rotational speed (2200 rpm) and friction pressure (60MPa).
- The fatigue fracture propagates from the inside out in the combined sample with low parameters (1800 rpm, 40 MPa and 6 s), but the fracture propagates inward from the surface in the samples with medium (2200 rpm, 40 MPa and 8 s) and high parameters (2200 rpm, 60 MPa and 10 s).

CONFLICT OF INTEREST

The authors declared no conflict of interest.

FINANCIAL DISCLOSURE

The authors declare that this study has received no financial support.

DECLARATION OF ETHICAL STANDARDS

The authors of this article declare that the materials and methods used in this study do not require ethical committee permission and/or legal-special permission.

REFERENCES

- [1] Crouch, I.G., Cimpoeru, S.J., Li, H., et al., (2017). The science of armour materials. Woodhead Publishing in Materials. 55-115.
- [2] U.S. Military Specification, (2009). MIL-DTL-12560J (MR), Armor plate, steel, wrought, homogeneous, U.S. Army Research Laboratory, Aberdeen Proving Ground.
- [3] U.S. Military Specification, (2008). MIL-DTL-46100E (MR), Armor plate, steel, wrought, high-hardness, U.S. Army Research Laboratory, Aberdeen Proving Ground.
- [4] U.S. Military Specification, (2009). MIL-DTL-32332 (MR), Armor plate, steel, wrought, ultra-high hardness, U.S. Army Research Laboratory, Aberdeen Proving Ground.
- [5] Nowacki, J. and Lukojc, A., (2005). Structure and properties of the heat-Affected zone of duplex steels welded joints. Journal Mater Process Technology, 164:1074-1081.
- [6] Ade, F., (1991). Ballistic qualification of armour steel weldments. Welding Journal, 70:53-54.
- [7] Kırık, İ., (2015). Effect of temperature on microstructure and mechanical behavior of diffusion bonded Armor 500 and AISI 1040 steels. Materials Testing, 57(4):296-300, DOI:10.3139/120.110716.
- [8] Sarsılmaz, F., Kırık, I., and Batı, S., (2017). Microstructure and mechanical properties of armor 500/AISI2205 steel joint by friction welding. Journal of Manufacturing Processes, 28:131-136.



-
- [9] Merzali, C., (2013). Improving the properties of the heat affected zone after welding in armor steels by heat treatment. Master's thesis. İstanbul Teknik Üniversitesi, Turkey.
- [10] Bekçi, M.L., Canpolat, B.H., Usta, E., et al., (2021). Ballistic performances of Ramor 500 and Ramor 550 armor steels at mono and bilayered plate configurations. *Engineering Science and Technology an International Journal*, 24:990-995.
- [11] Pakandam, F. and Varvani-Farahani, A., (2010). A comparative study on fatigue damage assessment of welded joints under uniaxial loading based on energy methods. *Procedia Engineering*, 2:2027-2035.
- [12] Teker, T. and Özdemir, N., (2012). Weldability and joining characteristics of AISI 430/ AISI 1040 steels using keyhole plasma arc welding. *The International Journal of Advanced Manufacturing Technology*, 63:1-4, DOI:10.1007/s00170-011-3890-5.
- [13] Cimpoeru, S.J., (2017). The mechanical metallurgy of armour steels, *Defence Science and Technology Group DST-Group-TR-3305*. (2016):1-32.
- [14] Crouch, I.G., Cimpoeru, S.J., Li, H., et al., (2017). Armour steels. *The Science of Armour Materials*, 55-115, DOI:10.1016/b978-0-08-100704-4.00002-5.
- [15] Nihal, Y., Yeliz, P., and Kubilay, A., (2013). Investigation of deformation characteristics of composite materials used in armor design. *Electronic Journal of Machine Technologies*, 10(4):1-21.
- [16] Taşkaya, S. and Gür, A.K., (2019). Investigation of the penetration balance of the wire feed speed in the weld metal in joining ramor 500 Armor Steel by Submerged Submerged Welding Method. *GÜFBED/GUSTIJ*, 9(3):444-453.
- [17] Özdemir, N., Sarsılmaz, F., and Haşçalık, A., (2007). Effect of rotational speed on the interface properties of friction-welded AISI 304L to 4340 steel. *Materials and Design*, 28:301-307.
- [18] Ali, G., Selçuk, B., and Mustafa, S.K., (2019). Effect of different arc welding processes on the metallurgical and mechanical properties of Ramor 500 armor steel. *Journal of Engineering Materials and Technology*, 142(2):1-23, DOI:10.1115/1.4045569.
- [19] Rajesh Jesudoss Hynes, N., and Shenbaga Velu, P., (2018). Microstructural and mechanical properties on friction welding of dissimilar metals used in motor vehicles. *Materials Research Express*, DOI:10.1088/2053-1591/aaabe6.
- [20] Lee, D.G., Jang, K.C., Kuk, J.M., et al., (2004). Fatigue properties of inertia dissimilar friction-welded stainless steels. *Journal Mater Process Technology*, 155-156:1402-1407.
- [21] Özdemir, N. and Orhan, N., (2005). Microstructure and mechanical properties of friction welded joints of a fine-grained hypereutectoid steel with 4%Al. *Journal of Materials Processing Technology*, 166(1):63-70, DOI:10.1016/j.jmatprotec.2004.07.095.
- [22] Adin, M.S. and Okumuş, M., (2021). Investigation of microstructural and mechanical properties of dissimilar metal weld between AISI 420 and AISI 1018 steels. *Arabian Journal for Science and Engineering*, DOI:10.1007/s13369-021-06243-w.
- [23] Mercan, S., Aydın, S., and Özdemir, N., (2015). Effect of welding parameters on the fatigue properties of dissimilar AISI 2205-AISI 1020 joined by friction welding. *International Journal of Fatigue*, 81:78-90.